AD-A138 040 AN INVESTIGTTION OF SOME BASIC PROPERTIES OF HYBRID COMPOSITE MATERIALS(U) DELAWARE UNIV NEWARK DEPT OF MECHANICAL AND AEROSPACE ENGINEE.. T W CHOU DEC 83 1/1

UNCLASSIFIED ARO-16666.21-EG DAAG29-80-K-0057 F/G 11/4 NL

END
FILMED
4-84
DTIC

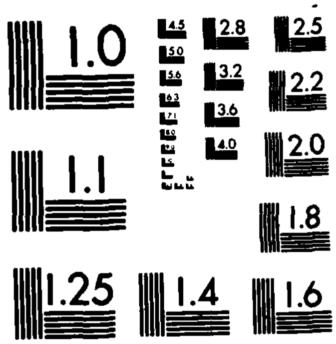

MICROCOPY RESOLUTION TEST CHART
NATIONAL BUREAU OF STANDARDS-1963-A

ARO 16666.21-EG

Unclassified

SECURITY CLASSIFICATION OF THIS PAGE (When Data Entered)

REPORT DOCUMENTATION PAGE		READ INSTRUCTIONS BEFORE COMPLETING FORM
REPORT NUMBER: Final Report	2. GOVT ACCESSION NO.	3. RECIPIENT'S CATALOG NUMBER
TITLE (and Subtitle): An Investigation of Some Basic Properties of Hybrid Composite Materials		5. TYPE OF REPORT & PERIOD COVERED: Final, 8/1/80-10/31/83
		6. PERFORMING ORG. REPORT NUMBER
AUTHOR(s): Tsu-Wei Chou		8. CONTRACT OR GRANT NUMBER(s): DAAG29-80-K-0057
9. PERFORMING ORGANIZATION NAME AND ADDRESS: Mechanical and Aerospace Engineering Department, University of Delaware, Newark, DE 19716		10. PROGRAM ELEMENT, PROJECT, TASK AREA & WORK UNIT NUMBERS
11. CONTROLLING OFFICE NAME AND ADDRESS: U. S. Army Research Office, Post Office Box 12211, Research Triangle Park, NC 27709		12. REPORT DATE: December, 1983
		13. NUMBER OF PAGES
14. MONITORING AGENCY NAME & ADDRESS (if different from Controlling Office)		15. SECURITY CLASS. (of this report): Unclassified
		15a. DECLASSIFICATION/DOWNGRADING SCHEDULE

16. DISTRIBUTION STATEMENT (of this Report)

Approved for public release; distribution unlimited.

DTIC ELECTE FEB 16 1984 A

17. DISTRIBUTION STATEMENT (of the abstract entered in Block 20, if different from Report)

18. SUPPLEMENTARY NOTES

The view, opinions, and/or findings contained in this report are those of the author(s) and should not be construed as an official Department of the Army position, policy, or decision, unless so designated by other documentation

19. KEY WORDS (Continue on reverse side if necessary and identify by block number)

Fiber composites, hybrids, fabrics, fabrication, testing, stiffness, strength

20. ABSTRACT (Continue on reverse side if necessary and identify by block number)

During the three years of this contract period, significant research results in hybrid composite materials have been accomplished in the areas of material fabrication, test method development, theoretical analyses of the stiffness and strength properties, as well as modelling the behavior of fabric composites. Altogether, seventeen technical papers have been published as a result of the research work. Some fundamental understandings of the mechanical behavior of hybrid composites have been achieved.

DD FORM 1473, 1 JAN 73 EDITION OF 1 NOV 65 IS OBSOLETE

UNCLASSIFIED

SECURITY CLASSIFICATION OF THIS PAGE (When Data Entered)

84 02 16 125

1. Forword

During the three years of this contract period, significant research results in hybrid composite materials have been accomplished in the areas of material fabrication, test method development, theoretical analyses of the stiffness and strength properties, as well as modelling the behavior of fabric composites. Altogether, seventeen technical papers have been published as a result of the research work. Some fundamental understandings of the mechanical behavior of hybrid composites have been achieved.

2. Table of Contents

A. An Outline of the Research Effort

We have made significant progress during the past two and one-half years in the fundamental understanding of hybrid composite behavior. Studies have been focused on the three geometric types of hybrids: interlaminated (interply), intermingled (intraply) and interwoven composites (Fig. 1).

To facilitate the presentation of our research results, it is useful to recapitulate an idealized stress-strain curve of interlaminated hybrid composites as shown in Fig. 2. The hybrid contains both high elongation (HE) and low elongation (LE) fibers. For composites with good bonding between the component phases, the stress-strain curve is given by OABC. The important features of this curve include the elastic behavior indicated by OA, the first cracking strain ε_{LU} associated with point A, the relatively flat portion of the curve AB, the successive rise of the curve at a smaller slope (BC) and the final failure strain of the hybrid given by the point D. The subscripts H and L are used to denote parameters related to high and low elongation fibers, respectively. The occurrence of first cracking (point A in Fig. 2) in the low elongation fibers at a strain level higher than that obtained when they are tested outside the composite (point A' in Fig. 2) is known as one form of the "hybrid effect". The extension of the curve between A and B at nearly constant stress is attributed to the multiple cracking of the LE fibers. The rise of the curve BC in Fig. 2 is attributed to the loading of the

high elongation fibers. The failure strain of the hybrid composite (D) is lower than that of high elongation fibers (G). This is because the multiple fracture of the LE fibers and partial debonding between the HE and LE fiber reinforced laminae.

The precise shape of the stress-strain curve of a hybrid composite depends upon the relative fiber volume fractions of the LE and HE fibers and their distribution in the composite. In the case of intermingled hybrid composites, multiple fractures of the LE fibers can take place over a wide range of the stress-strain curve and at increasing applied load.

The above brief introduction points out several areas of basic interest in hybrid composite research. They include the fabrication of intermingled and interlaminated composites, the elastic behavior, hybrid effect, multiple fiber fracture and ductility or final failure strain of the hybrid composite. Research results on these items will be discussed in Secs. B-E. Interwoven hybrid composites will be discussed in Sec. F and the general continuum mechanics problems of composites are given in Sec. G.

B. Hybrid Material Fabrication, Characterization and Test Method Development

(1) Hybrid Material Fabrication

A major goal of this research program is to assess the effect of fiber dispersion and mixing on the performance of the hybrid composite. Thus, it is essential to examine the full range of fiber arrangements, from interlaminated and intermingled constructions to interwoven laminae. Among these three types,

the intermingled arrangement is most difficult to make because the degree of fiber mixing can vary from the mixture of large diameter tows to the uniform dispersion of individual filaments. From the viewpoint of basic research, the mixing of filaments cannot be ignored, and it is one of the key efforts in the experimental program.

Because of the sizing and coatings on the filaments as well as the tangling of the filaments in a fiber tow it was extremely difficult to achieve intimate fiber mixing. Various techniques, including the use of liquid jet, air jet and other mechanical means were attempted. Finally, a specially designed filament winding technique was successfully developed to fabricate intermingled hybrid composites by mixing Kevlar and glass filaments in a phenolic resin. Excellent dispersion and distribution of the filaments have been achieved [1]. Test results of these materials are discussed in Sec. III C.

(2) Test Method Development

During the course of the mechanical property testing effort, it was felt that the conventional honeycomb sandwich beam compression testing technique has certain disadvantages, such as its high cost and the large amount of material used to fabricate the sandwich faces. Efforts were then devoted to develop the concept for design and fabrication of a <u>reusable</u> sandwich beam for compression tests. With the co-operation of Professor Overbeeke of Eindhoven University of Technology a reusable sandwich beam has been successfully developed and tested. Besides being reusable, the design also has the following advantages: excellent specimen

-load alignment, large specimen guage length (2") and high reproducibility in test results. The beam design is shown in Fig. 3 and details of hybrid composite compression test results are documented in Ref.[2].

C. Elastic Properties

The study of elastic behavior is basic to the understanding of the performance of hybrid composites. A major development in this research is the establishment of analytical technique for predicting elastic moduli of multiphase short-fiber composites [3]. Both self-consistent and bound approaches are adopted. In the bound method, closed form solutions have been obtained for the upper and lower bounds of the effective elastic moduli of unidirectional short-fiber composites. The short-fibers are modeled by aligned ellipsoidal inclusions of the same aspect ratio but not necessarily the same size. We adopt a perturbation expansion of the composite local strain field by using the Green's function tensor. Explicit expressions of the effective elastic moduli are derived up to the third order term by use of the information on the correlation functions. The variational method is then employed to optimize the bounds of the effective modulus in a closed form.

The present approach predicts narrower bounds than those of Hashin and coworkers for the limiting cases of binary composites containing spherical particles and continuous fibers since their bounds correspond to a model that takes the correlation functions up to the second order into account. Figure 4 shows such a comparison. Furthermore, the present approach is not

limited by the number of component phases in a composite. Figure 5 gives an example of the theoretical prediction of transverse Young's modulus as a function of relative fiber volume fraction in a Kevlar/glass/epoxy system. Experimental data are obtained from Ref. [1].

D. Stress Concentrations and Hybrid Effect

In order to better understand the hybrid effect as depicted in Fig. 2, we choose to explain this interesting phenomenon from the view point of stress redistributions in hybrid composites.

(1) Stress Concentrations

Both static and dynamic stress concentration factors have been examined and major conclusions are outlined below.

(a) Static Stress Concentrations [4,5]

An intermingled hybrid composite sheet containing both high elongation and low elongation fibers arranged in alternating positions is shown in Fig. 6a. Stress concentration factors for both types of fibers immediately adjacent to a group of fractured fibers have been evaluated. The method of influence function and Fourier series representation are adopted. Results of stress concentration factors are presented in terms of the number of fractured fibers and their geometric arrangements as shown in Fig. 6b. The analysis demonstrates that, as compared to the case of pure low elongation fiber composites, there is a reduction of the stress concentration factor of the low elongation fibers when they are dispersed among the high elongation fibers. The implications of this finding is discussed in Sec. D(3).

(2) Dynamic Stress Concentrations [6]

A theoretical analysis has been performed to evaluate the dynamic stress concentration factor in a simple interlaminated hybrid composite (Fig. 7). The governing equation of the shear-lag analysis is solved by a combination of Laplace transform, influence function technique and Fourier series representation.

At the fracture of a low elongation (LE) fiber, the present model predicts two stress waves propagating along each fiber in the hybrid. The phase difference of the dynamic responses contributed by these waves at the middle section of a fiber immediately adjacent to a fiber breakage is controlled by the fiber mass per unit length. The magnitude of dynamic responses are determined by the fiber extensional stiffness. Figure 8(a) depicts the time variation of stress concentration components K_1 and K_2 due to the two types of fibers. The resultant of K_1 and K_2 is also shown. When the two layers of fibers in Fig. 7 are identical the hybrid is reduced to an ordinary binary system and the two stress waves become in-phase as shown in Fig. 8(b). It can be shown that the parent LE fiber composite always provides the upper bound for stress concentration of hybrid.

(3) Hybrid Effect [4-6]

The term "hybrid effect" may mean different phenomena for different investigators. Here we focus on the effect indicated by points A and A' on Fig. 2, and the explanation is based upon the above stress analyses. In the dynamic analysis, the fiber dynamic stress response is consisted of two stress waves always out-of-phase in a hybrid with fibers of different mass and

elastic stiffness. This fact suggests that the resultant stress concentration on the LE fibers of a hybrid composite is always lower than that in the pure LE fiber composite. A similar conclusion was obtained in the static stress concentration analysis.

Thus, it can be expected that the LE fibers in a hybrid can carry higher load than those in a pure LE fiber composite, and an increment in failure strain can be expected. Qualitative comparisons of experimentally measured hybrid effects and theoretical predictions are given in Refs. [4-6] and the validity of the present approach has been clearly demonstrated.

E. Statistical Strength Theory [7-9]

Another form of hybrid effect has been observed regarding the ultimate failure strain and damage tolerance of composites. It has been demonstrated both theoretically and experimentally that the ultimate failure strain of a pure LE fiber composite is enhanced if some of the LE fibers are replaced by HE fibers. The dispersion of LE fibers among the HE fibers has the effect of enhancing multiple fractures of the LE fibers. Local damage of the LE fibers at the proper relative fiber volume fraction can be constrained by the HE fibers. As a result of this synergistic effect, fiber damage propagates in a progressive manner and the ultimate failure strain of the hybrid is higher than that of the corresponding LE fiber composite.

A theoretical analysis has been performed to predict the stress-strain curve of an intermingled hybrid composite taking into account the statistical strength distribution of the component fibers. Figure 9 depicts a simple five-fiber model taken from a composite infinite in size. The strength of fibers is

assumed to follow a truncated normal distribution. The ratio of ultimate failure strains of the HE and LE fibers is 3. A Monte Carlo simulation is adopted to predict the composite strength. The composites are treated as bundles of links, as indicated by the "0" in Fig. 9. Under an applied load , the weakest link in the composite model fails first, and the resulting stress concentration is computed imme ately. This determines the location of the next link to fail. ᵉe failure sequences of fiber links are given by the Arabic nun s in Fig. 9(a) and (b) for LE composite and hybrid, respectively. Figure 10 gives the predicted stress-strain curves of LE, HE and LE/HE hybrid composites where the LE and HE fibers are assumed to have the same ultimate strength. Much more extensive predictions of the stress-strain relation can be readily achieved by using higher number of fibers. The theoretical curve of the hybrid composite coincide remarkably well with experimental results at least in a qualitative fashion.

The progressive nature of damage propagation in Figs. 9(b) and 10 clearly demonstrate the desirable effect of hybridization. The ductility of LE fiber composites can be enhanced by selectively replacing the brittle fibers with more ductile ones, and the resulting stress-strain curve resembles that of a ductile metal.

F. Fabric Composites [10-17]

Woven fabrics are now considered to be a more important reinforcing material in the composite technology than a decade ago. The understanding of the reinforcing mechanics in fabric

composites, however, has not been fully established yet. Although the structural efficiency of fabric composites is not as high as that of the unidirectional laminates, their versatile properties and low fabrication costs have made fabric composites attractive for structural applications.

(1) Fabric Structures

Most woven fabrics are formed by interlacing two sets of threads, the warp and the fill as shown in Fig. 11. The types of fabrics can be identified by the repeating patterns. Two geometrical parameters are defined first for identification; n_{fg} denotes that a warp thread is interlaced with every n_{fg}-th fill thread and n_{wg} denotes that a fill thread is interlaced with every n_{wg}-th warp thread. Here, we focus our attention on the case of $n_{wg} = n_{fg} = n_g$. Fabrics with $n_g \geq 4$ and with isolated interlaced regions are known as satin weaves, and fabrics with $n_g = 2$ are known as plain weaves. Figure 12d depicts an 8 harness ($n_g = 8$) hybrid fabric. In the case of hybrid fabrics, parameters which define the material arrangements need to be specified. For example, $n_{fm} = 4$ and $n_{wm} = 4$ indicate, respectively, the pattern of arrangement of fiber types in the fill direction repeats for every four warp threads and the pattern in the warp direction repeats for every four fill threads where subscript m signifies a material parameter. Two implicit assumptions are adopted; no spacing between threads are allowed and hybrid fabrics consist of only two material types, denoted by α and β.

(2) Analytical Models

For the purpose of analyzing different types of fabric composites and several thermomechanical properties, four analytical models have been developed. In the first model, known as the mosaic model, a fabric composite is idealized as an assemblage of asymmetrical cross-ply laminates (Fig. 12a). Based upon the assumptions of iso-stress and iso-strain, bounds of elastic moduli are derived and they provide an approximate method for predicting the elastic moduli and the results compare fairly well with experimental measurements.

In the second method, the mosaic model is modified to take into consideration the effect of fiber undulation and continuity on composite stiffness (Fig. 12b). A one-dimensional strip of the fabric composite forms the basis of the analysis and the classical laminated plate theory is applied to each infinitesimal piece of the composite plate. The predictions of this model show good agreement with two-dimensional finite element results. This approach, combined with some simple assumptions, has been extended to investigate the bi-linear or "knee" behavior of the stress-strain relations of plain weave composites. The results compare favorably with those obtained by other investigations.

The concept of the third model is developed based on the findings of load transfer in satin weave composites. The region with straight threads surrounding an undulated interlaced region has higher local in-plane stiffness than the latter and acts as a load-transferring bridge (Fig. 12c). Numerical results of elastic moduli of graphite/epoxy exhibit a good agreement with experiments. This model has also been extended to the analysis

of the knee behavior in satin weave composites. The predicted stress-strain curve shows an excellent correlation with the experimental curve for glass/polyimide 8 harness satin composites.

The fourth model, which is referred to as the "modified bridging model," is specially developed for treating hybrid woven composites (Fig. 12d). The basic idea of the bridging action of the third model is preserved, although the geometry of this fourth model is much involved due to the complexity in the hybrid fabric structure. This model provides a significant improvement of the predictions of the simple bound results and gives results very close to the experimental measurements of stiffness (Fig. 13).

The above models have been applied to predict the in-plane thermal expansion coefficients of hybrid and non-hybrid fabric composites. Finally, the non-linear material behavior of fabric composites also have been examined.

G. Continuum Mechanics of Inhomogeneity Problems [21]

When an elastic inhomogeneity and its surrounding solid are exposed to different changes in their thermal conditions within the limits of the linear theory of elasticity, thermal stress concentrations result around the inhomogeneity. It is shown in this work that if the thermal stresses just inside an arbitrarily shaped anisotropic inhomogeneity embedded in a different anisotropic solid are known, the corresponding thermal stresses just outside the inhomogeneity are directly deducible. Likewise, it is found that the specification of the thermal gradient just inside such an arbitrary inhomogeneity enables one to deduce the

corresponding thermal gradient just outside the inhomogeneity. This result, in turn, enables us to show that the thermal gradient produced within any internal or external thin thermo-insulating coating is the same as the thermal gradient on the other side of the coating. An exact closed solution is then given for an isotropic inhomogeneity in the shpae of a general hyperellipsoid by reformulating the thermoelastic problem in the form of an equivalent transformation strain problem, and then taking advantage of Eshelby's (1957) elegant equivalent inclusion method. It is found that an undisturbed temperature field which is a polynomial of degree N in the Cartesian coordinates induces within the inhomoegenity stresses and strains which are polynomials of exactly the same degree as the undisturbed temperature field. Explicit formulae are given for the thermal stress concentrations, the total elastic energy associated with the inhomogeneity, and the change in volume of the inhomogeneity. It is found that the volume change or an arbitrarily shaped inhomogeneity is proportional to the volume integral of the difference of effective elastic strain within the inhomogeneity and the equivalent homogeneous inclusion. If the inhomogeneity and matrix differ only in their conductivity and thermal expansion coefficients, then the desired volume change is proportional simply to the averaged temperature distribution within the inhomogeneity, with no contribution from the thermal stresses.

H. Summary

During the past three years, the following major accomplishments have been made:

(1) Significant research results in hybrids have been obtained in material fabrication, theoretical analyses of the stiffness and strength properties, and modelling the behavior of fabric composites.

(2) Seventeen technical papers have been published as a result of the research work.

(3) Research results also have been presented at the following national and international conferences:

a) First Japan-US Conference on Composite Materials, Tokyo, 1981

b) US National Congress of Theoretical and Applied Mechanics, Ithaca, 1982

c) Fourth International Conference of Composite Materials, Tokyo, 1982 (two papers)

d) Army Workshop on "Advancements in Hybrid Composite Materials"

e) ASME Winter Annual Meeting, Phoenix, 1982

(4) T. W. Chou served as the Organizer of the Research Workshop on "Advancements in Hybrid Composite Materials," sponsored by the Army Research Office and held on 9-10 November 1982 in West Palm Beach, Florida.

(5) Research results obtained in 1981-92 were cited by the Army Research Office as having achieved "distinguished" accomplishments.

(6) Participating Scientific Personnel

(a) Graduate Students

M. Gruber: M.S., Mechanical & Aerospace Engineering Dept.

S. Nomura: Ph.D., Mechanical & Aerospace Engineering Dept.

(b) Undergraduate Student

D. Jeskee: B.S., Mechanical & Aerospace Engineering Dept.

(c) Research Associates

H. Fukuda

T. Ishikawa

H. Fukunaga

(d) Visiting Scholar

X. Ji

I. Bibliography

1. M. Gruber and T. W. Chou, "Elastic Properties of Intermingled Hybrid Composites," Polymer Composites, 4, 265 (1983).

2. M. Gruber, J. Overbeeke and T. W. Chou, "A Reusable Sandwich Beam for Composite Compression Test," J. Comp. Mat, 16, 162 (1982).

3. S. Nomura and T. W. Chou, "Bounds of Elastic Moduli of Short-Fiber Composites," J. Appl. Mech., in press.

4. H. Fukuda and T. W. Chou, "Stress Concentrations Around a Discontinuous Fiber in a Hybrid Composite Sheet," Trans. Japan Society for Composite Materials, 7, 37 (1982).

5. H. Fukuda and T. W. Chou, "Stress Concentrations in a Hybrid Composite Sheet," J. Appl. Mech., in press.

6. X. Ji, G. Hsiao and T. W. Chou, "A Dynamic Explanation of the Hybrid Effect," J. Comp. Mat., 15, 443 (1981).

7. H. Fukuda and T. W. Chou, "Monte Carlo Simulation of the Strength of Hybrid Composites," J. Comp. Mat., 16, 371 (1982).

8. H. Fukuda and T. W. Chou, "Stiffness and Strength of Hybrid Composites," Composite Materials: Mechanics, Mechanical Properties and Fabrication, Japan Society for Composite Materials, Tokyo, Japan, p. 78, (1981).

9. H. Fukuda and T. W. Chou, "A Statistical Approach to the Strength of Hybrid Composites," Proceedings of the Fourth International Conference on Composite Materials, p. 821, (1982).

10. T. Ishikawa and T. W. Chou, "Elastic Behavior of Woven Hybrid Composites," J. Comp. Mat., 16, 2 (1982).

11. T. Ishikawa and T. W. Chou, "One-dimensional Analysis of Woven Fabric Composites," AIAA Journal, 21, 1714 (1983).

12. T. Ishikawa and T. W. Chou, "Stiffness and Strength Behavior of Woven Fabric Composites," J. Mat. Sci., 17, 3211 (1982).

13. T. Ishikawa and T. W. Chou, "In-plane Thermal Expansion and Thermal Bending Coefficients of Fabric Composites," submitted to J. Comp. Mat., 17, 92 (1983).

14. T. Ishikawa and T. W. Chou, "Thermo-mechanical Analysis of Hybrid Fabric Composites," J. Mat. Sci., 18, 2260 (1983).

15. T. Ishikawa and T. W. Chou, "Nonlinear Behavior of Woven Fabric Composites," submitted to J. Comp. Mat., 7, 399 (1983).

16. T. Ishikawa and T. W. Chou, "Stiffness and Strength Properties of Woven Fabric Composites," Proceedings of the Fourth International Conference on Composite Materials, p. 489, (1982).

17. T. Ishikawa and T. W. Chou, "In Plane Thermal Expansion and Thermal Bending Coefficients of Fabric Composites," in Advances in Aerospace Structures and Materials, ASME, New York, p. 115, (1982).

J. Figure Captions

Fig. 1. (a) Interlaminated, (b) Intermingled, and (c) Interwoven hybrid composites.

Fig. 2. A typical stress-strain curve of an interlaminated hybrid composite.

Fig. 3. (a) Dimensions of the reusable sandwich beam without clamps, (b) The reusable sandwich beam.

Fig. 4. G_{12}^* vs. V_f. ——: bound approach, ----: self-consistent approach, ——·——·——·——: Hashin and Strikman's result.

Fig. 5. Transverse effective Young's modulus E_{22}^* vs. relative fiber volume fraction of an intermingled Kevlar/glass hybrid composite. Total fiber volume fraction = 65% and E_m denotes matrix Young's modulus.

Fig. 6a. Fiber arrangement in an intermingled hybrid composite. (LM: low elastic modulus and high elongation, HM: high elastic modulus and low elongation).

Fig. 6b. Fiber stress concentrations as functions of the number of discontinuous fibers. A, B, C, D, E and F indicate locations in Fig. 5. $E^*A^*/EA = 1/3$.

Fig. 7. A model of hybrid composite.

Fig. 8. (a) Variation of stress-concentration factor. ($m^*/m = 6$, $E^*A^*/EA = 1$, $d^2/h^2 = 1$), (b) Variation of stress concentration factor. ($m^*/m = 2$, $E^*A^*/EA = 1$, $d^2/h^2 = 1$).

Fig. 9. Examples of failure process. (a) Non-hybrid composite, (b) Hybrid composite.

Fig. 10. Normalized stress-strain relations of non-hybrid and hybrid composites.

Fig. 11. Fabric geometries.

Fig. 12. (a) Mosaic model, (b) Fiber undulation model, (c) Bridging model, (d) Modified bridging model.

Fig. 13. In-plane stiffness vs. relative fiber volume fraction of a graphite/Kevlar hybrid fabric composite. Total fiber volume fraction is 60%.

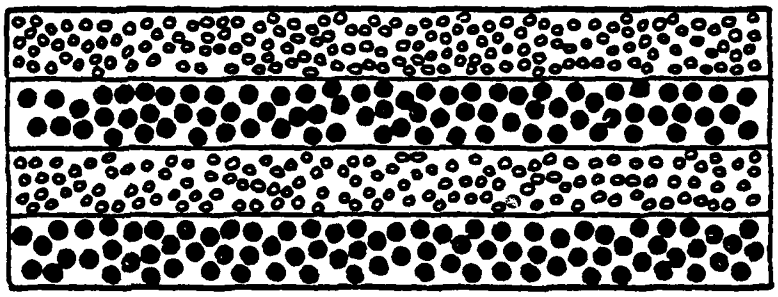

(a)

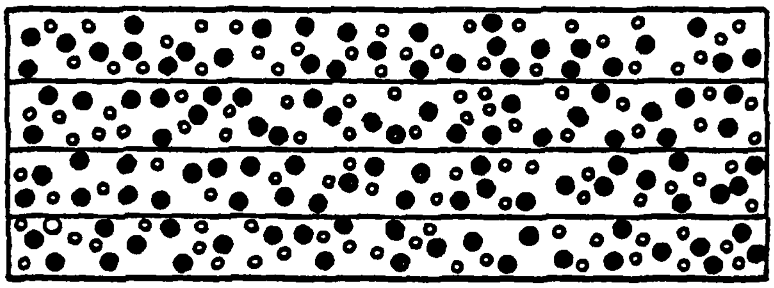

(b)

Fig. 1

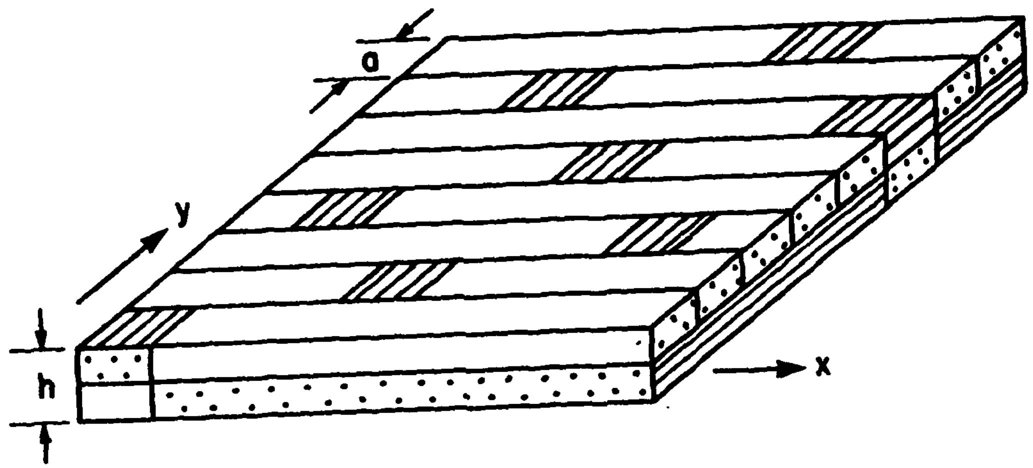

(c)

Fig. 1

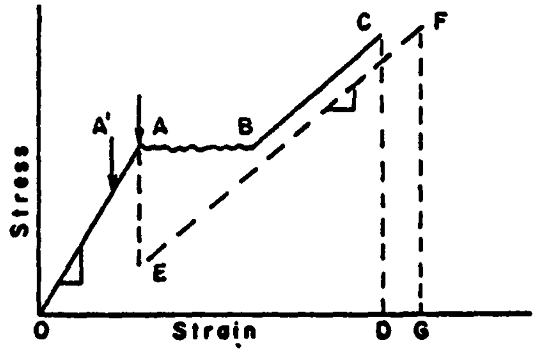

Fig. 2

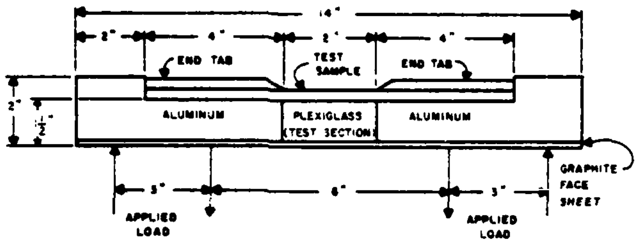
14"
2"
4"
2"
4"
END TAB
TEST SAMPLE
END TAB
2"
1/2"
ALUMINUM
PLEXIGLASS (TEST SECTION)
ALUMINUM
GRAPHITE FACE SHEET
3"
6"
3"
APPLIED LOAD
APPLIED LOAD

(a)

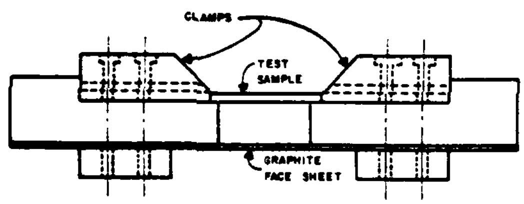
CLAMPS
TEST SAMPLE
GRAPHITE FACE SHEET

(b)

Fig. 3

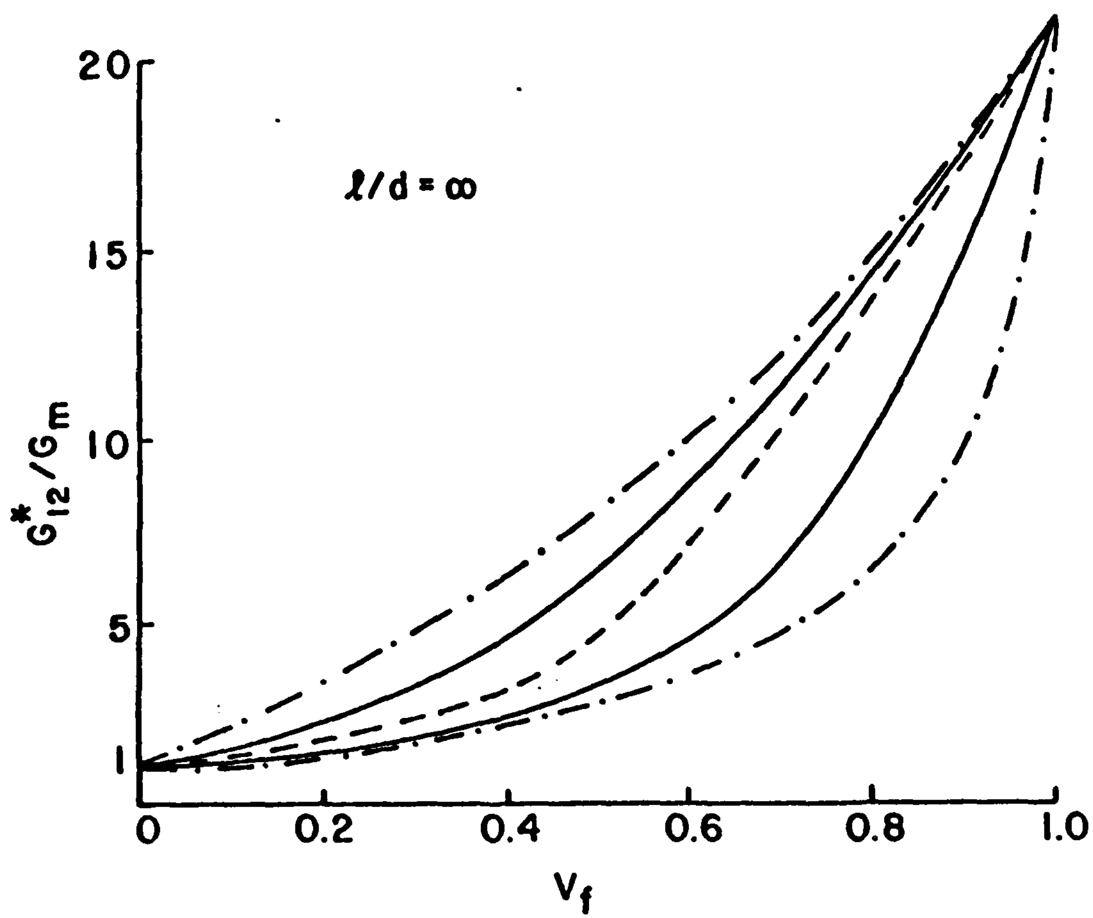

Fig. 4

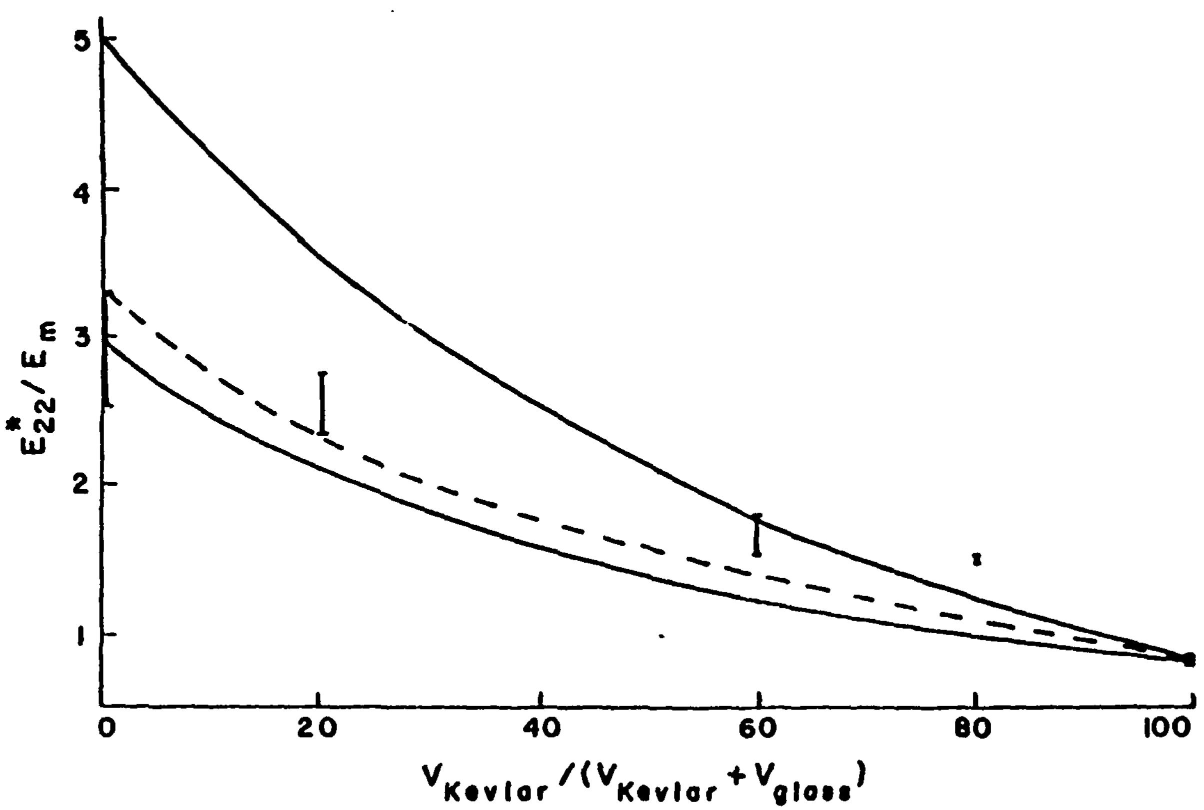

Fig. 5

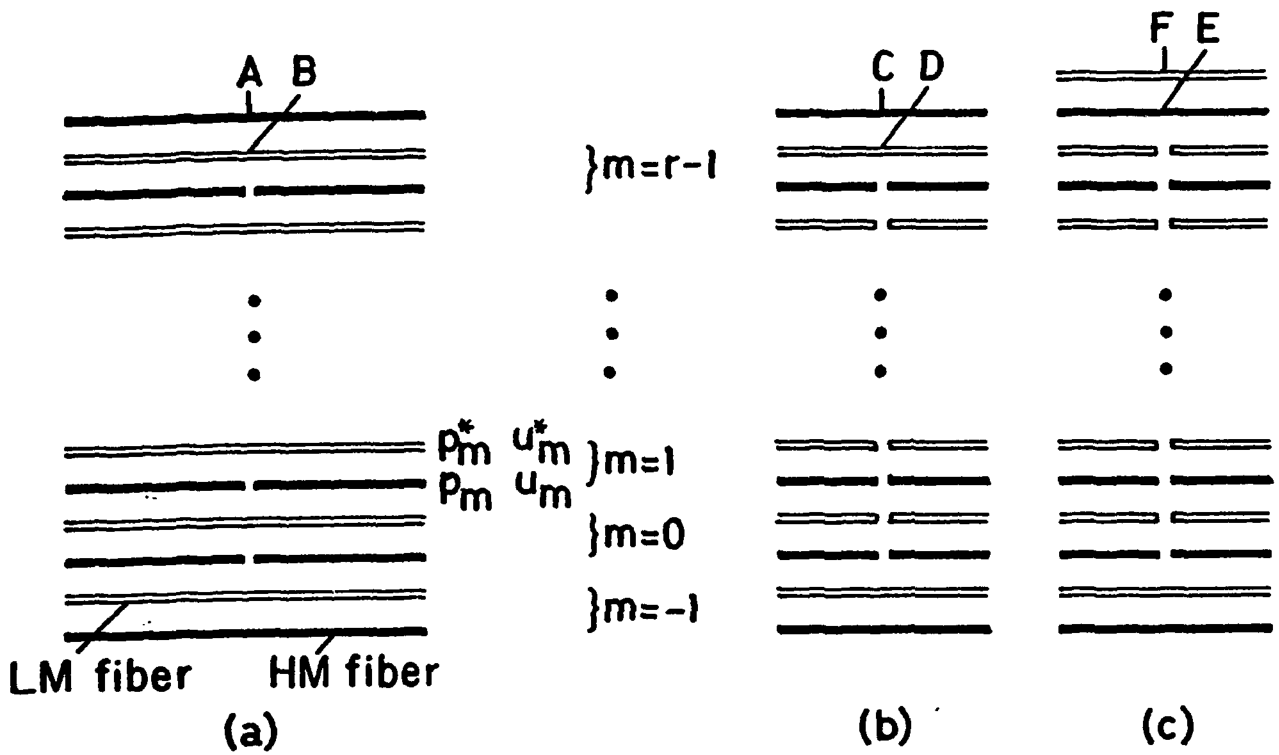

Fig. 6a

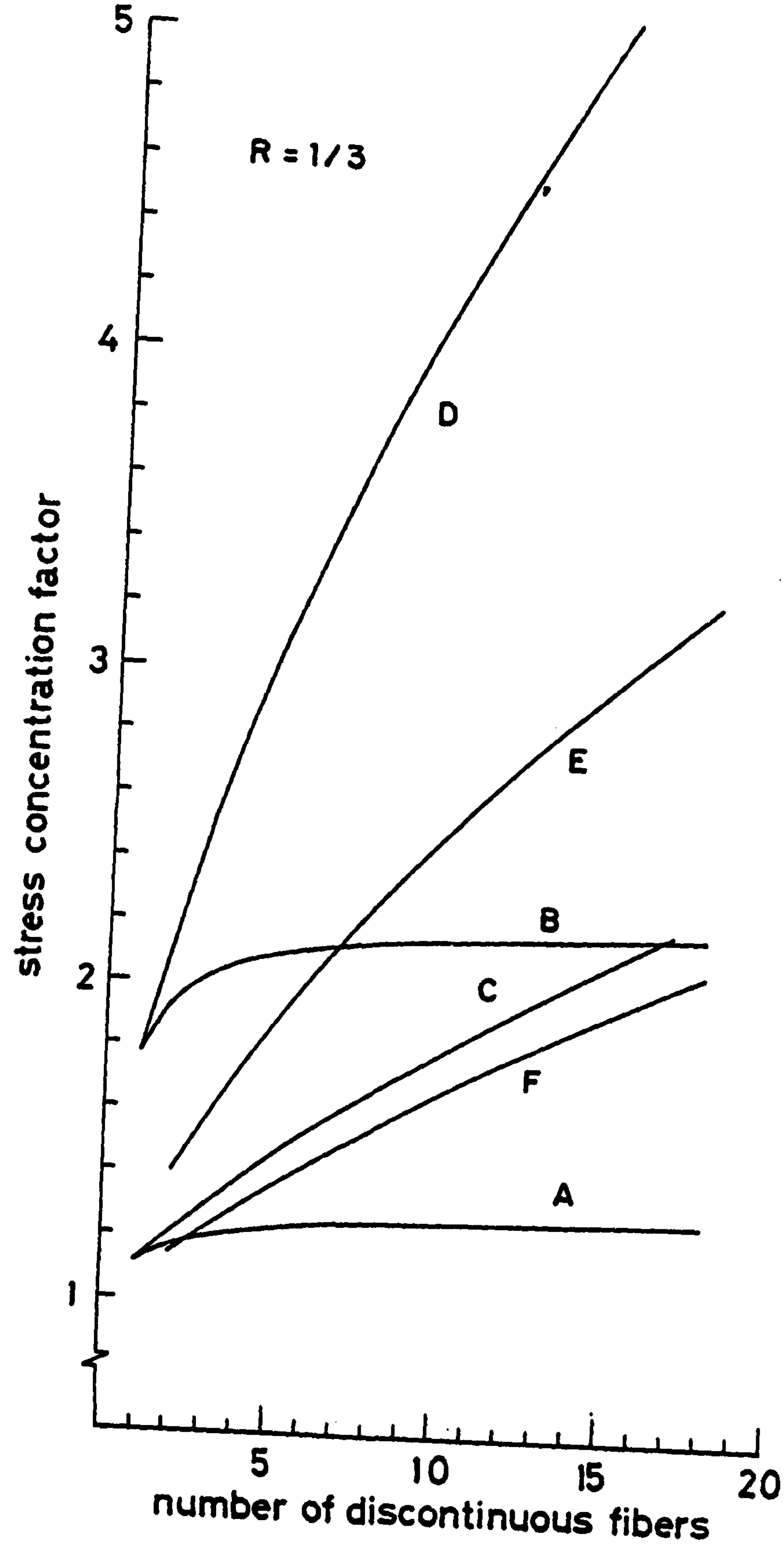
R = 1/3
stress concentration factor
number of discontinuous fibers
5
4
3
2
1
5
10
15
20
D
E
B
C
F
A

Fig. 6b

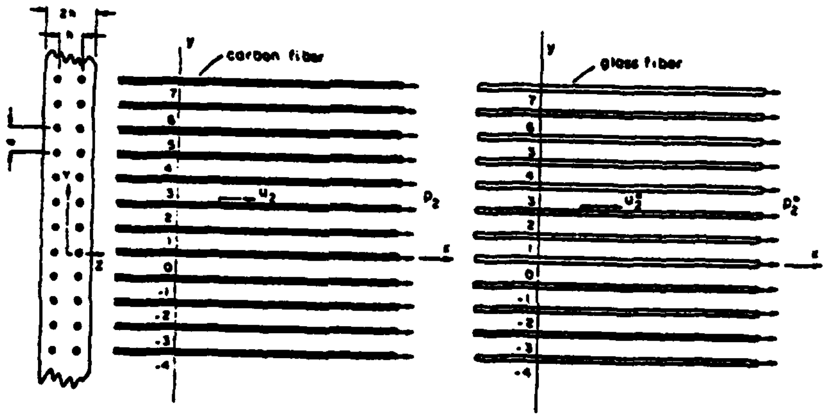

Fig. 7

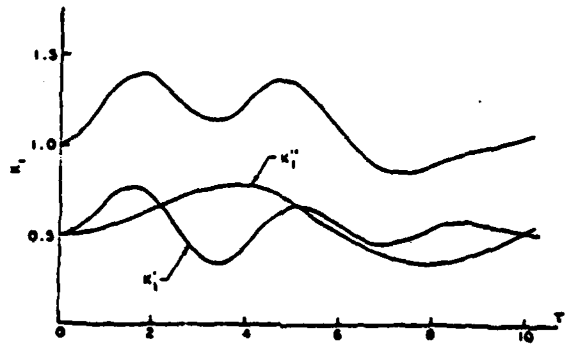
1.5
1.0
0.5
K_I
K_I''
K_I'
0
2
4
6
8
10
T

(a)

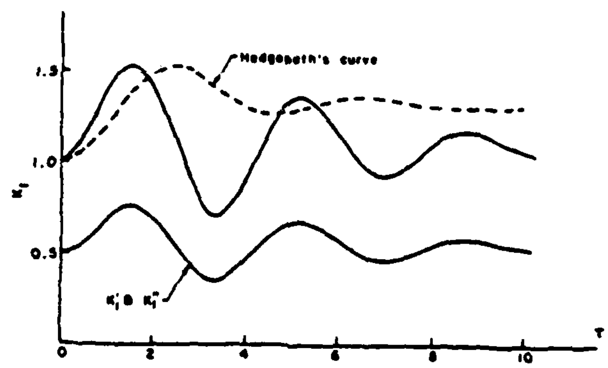
Hedgepeth's curve
1.5
1.0
0.5
K_I
K_I' & K_I''
0
2
4
6
8
10
T

(b)

Fig. 8

0	0	0	0	0
0	0	0	0	0
0	0	0	0	0
0	0	0	0	0
0	0	0	2	0
0	0	0	0	0
0	0	0	0	0
0	0	0	0	0
0	0	0	0	0
0	0	0	0	0
0	0	0	0	0
0	0	0	0	0
0	0	0	0	0
3	1	4	5	6
0	0	0	0	0
0	0	0	0	0
0	0	0	0	0
0	0	0	0	0
0	0	0	0	0
0	0	0	0	0

(a)

0	0	0	0	0
0	0	0	0	2
0	0	0	0	0
0	0	0	0	0
0	0	0	0	0
0	0	0	0	0
10	0	13	0	14
0	0	11	0	0
3	0	4	0	0
7	16	8	15	1
0	0	0	0	0
9	0	0	0	0
0	0	0	0	0
0	0	0	0	0
0	0	0	0	0
0	0	0	0	0
0	0	0	0	0
0	0	0	0	0
0	0	0	0	0
12	0	6	0	5
LE	HE	LE	HE	LE

(b)

Fig. 9

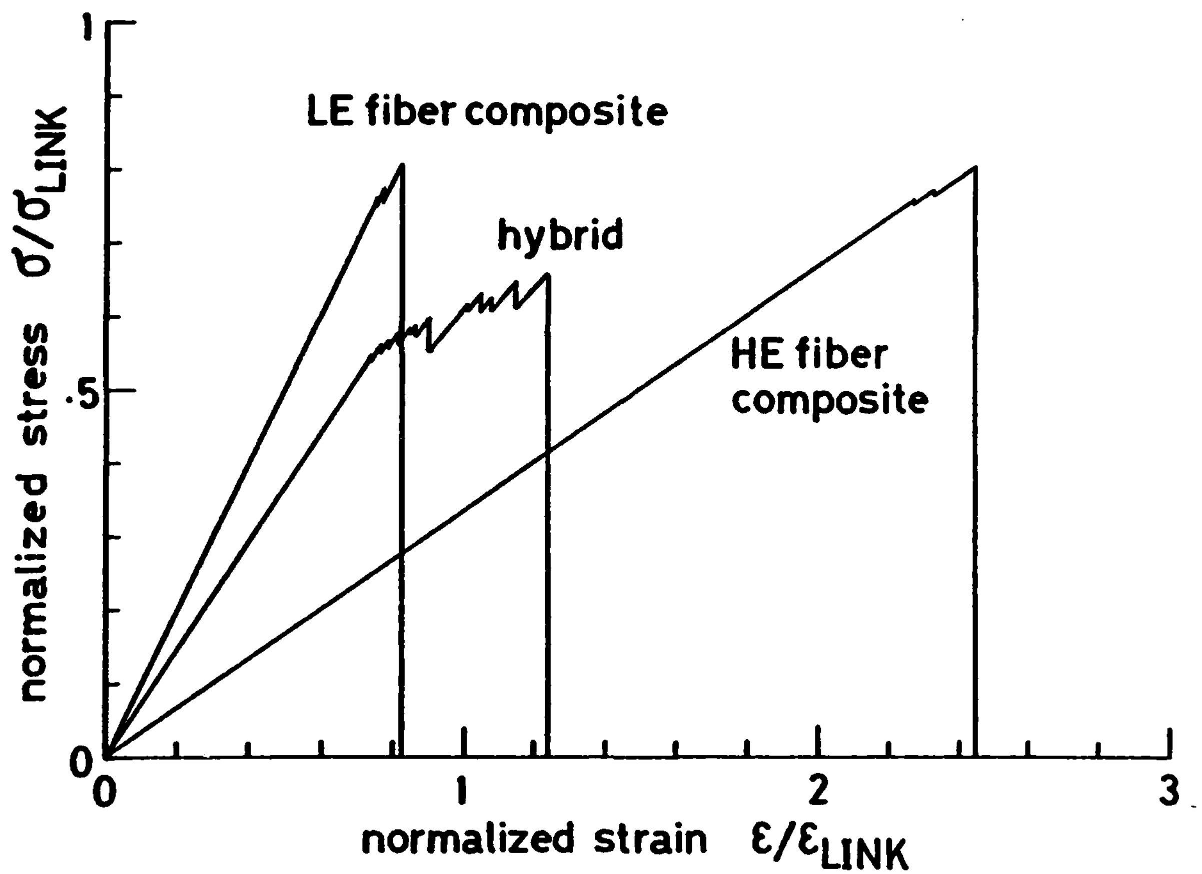

LE fiber composite
hybrid
HE fiber composite
normalized stress σ/σ_{LINK}
normalized strain $\varepsilon/\varepsilon_{LINK}$
0
.5
1
0
1
2
3

Fig. 10

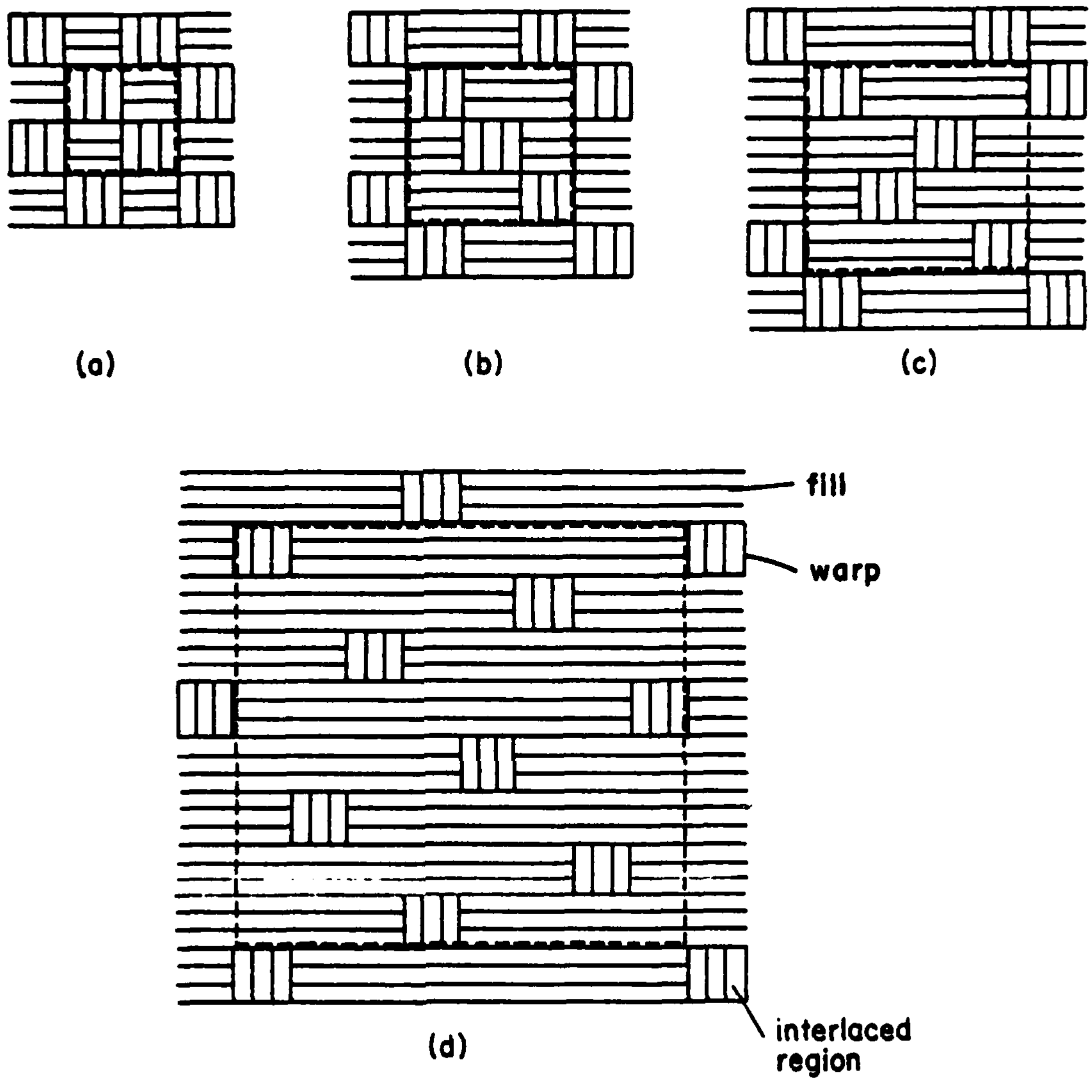

Fig. 11

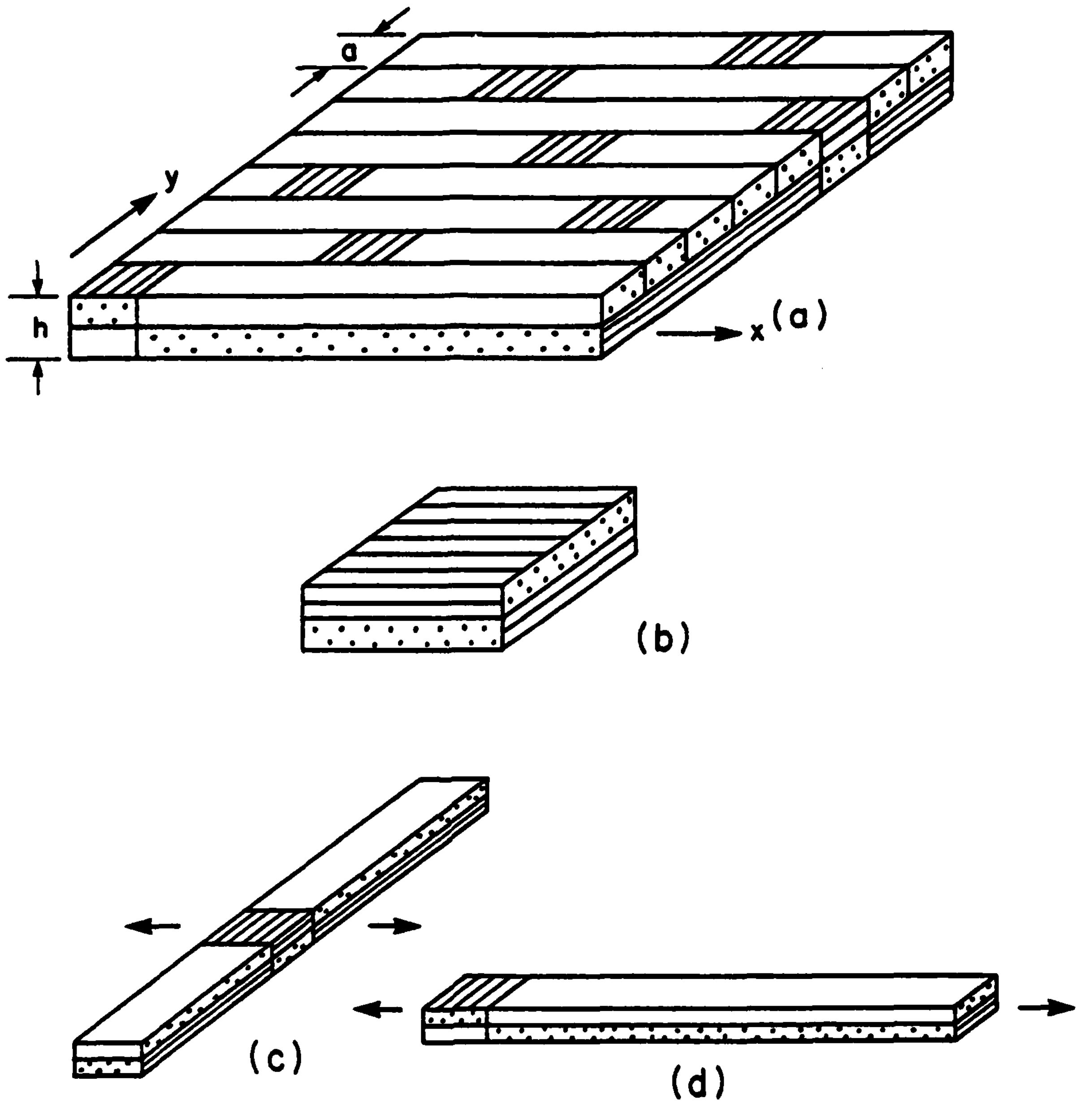

Fig. 12a

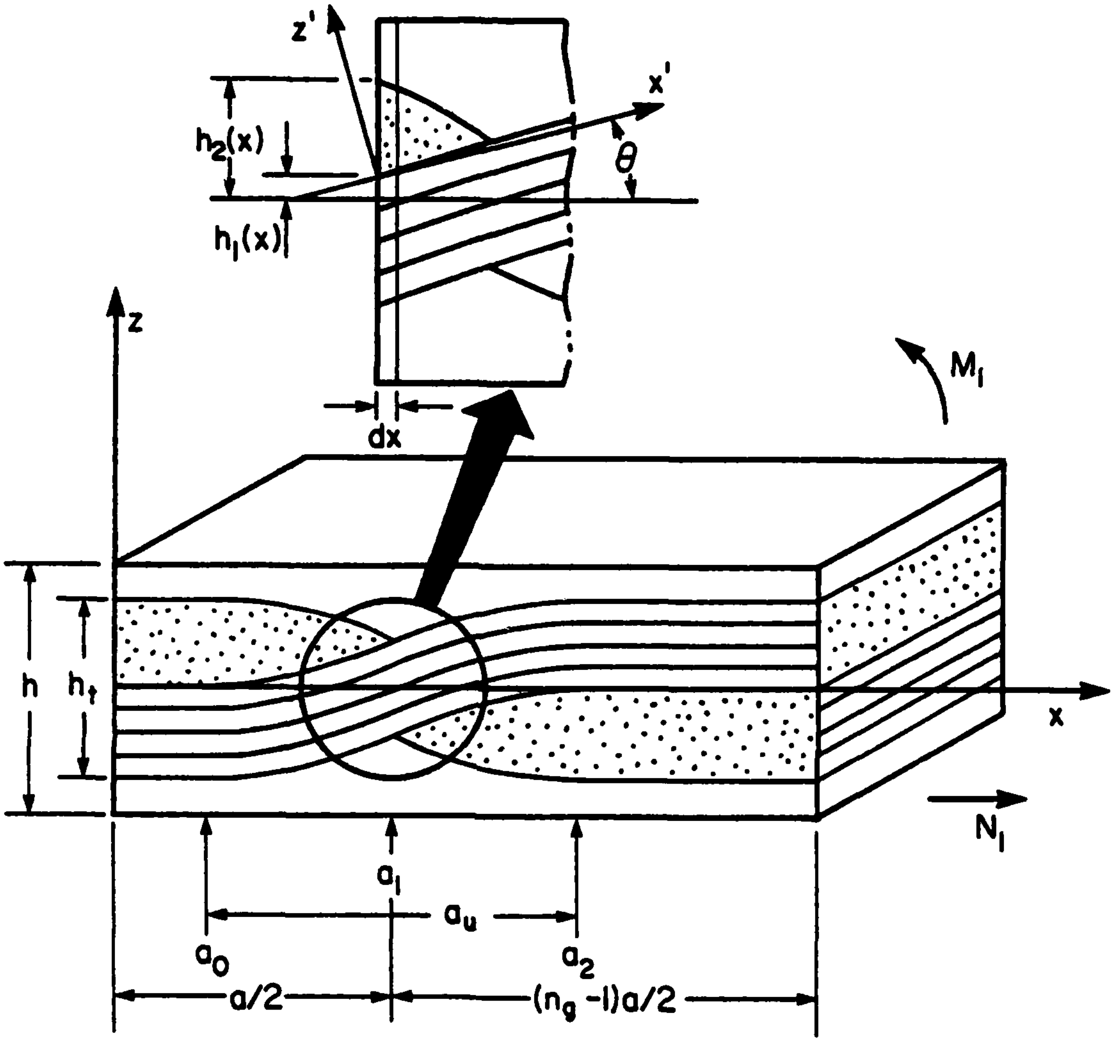

Fig. 12 b

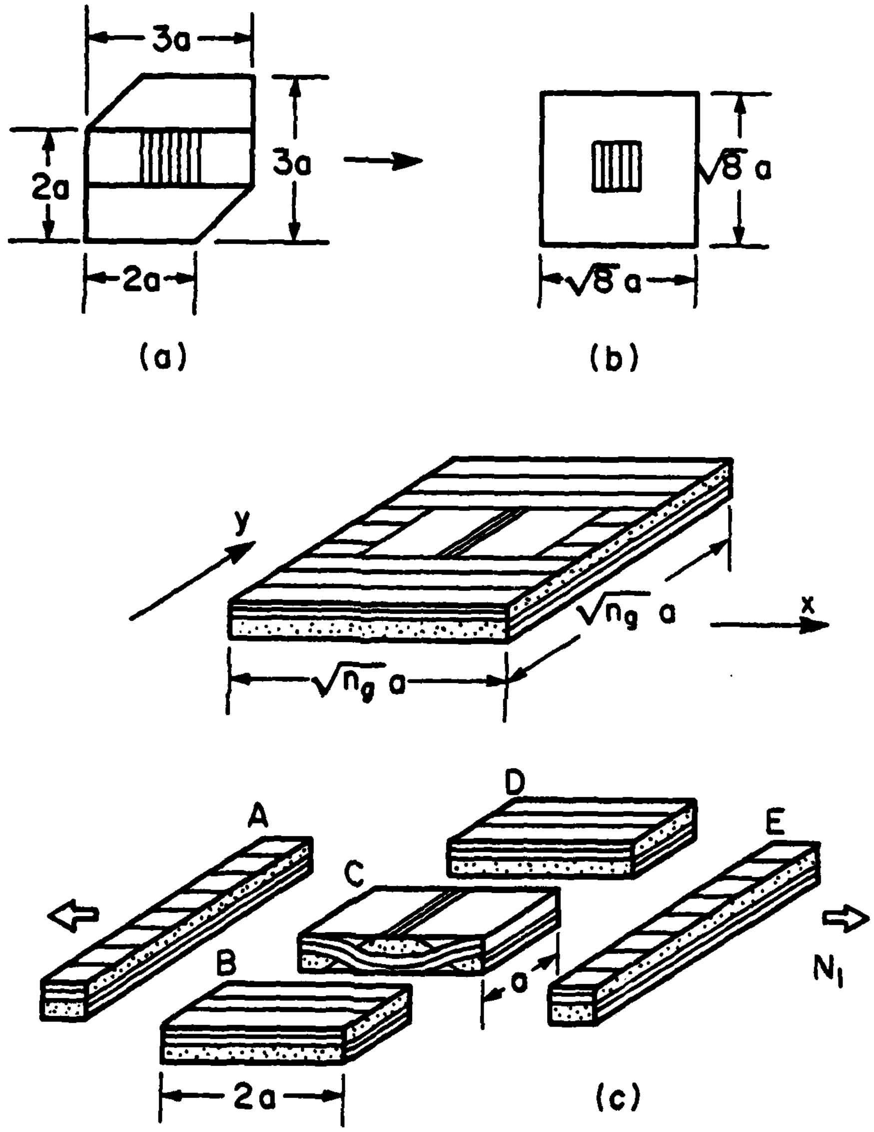

Fig. 12 C

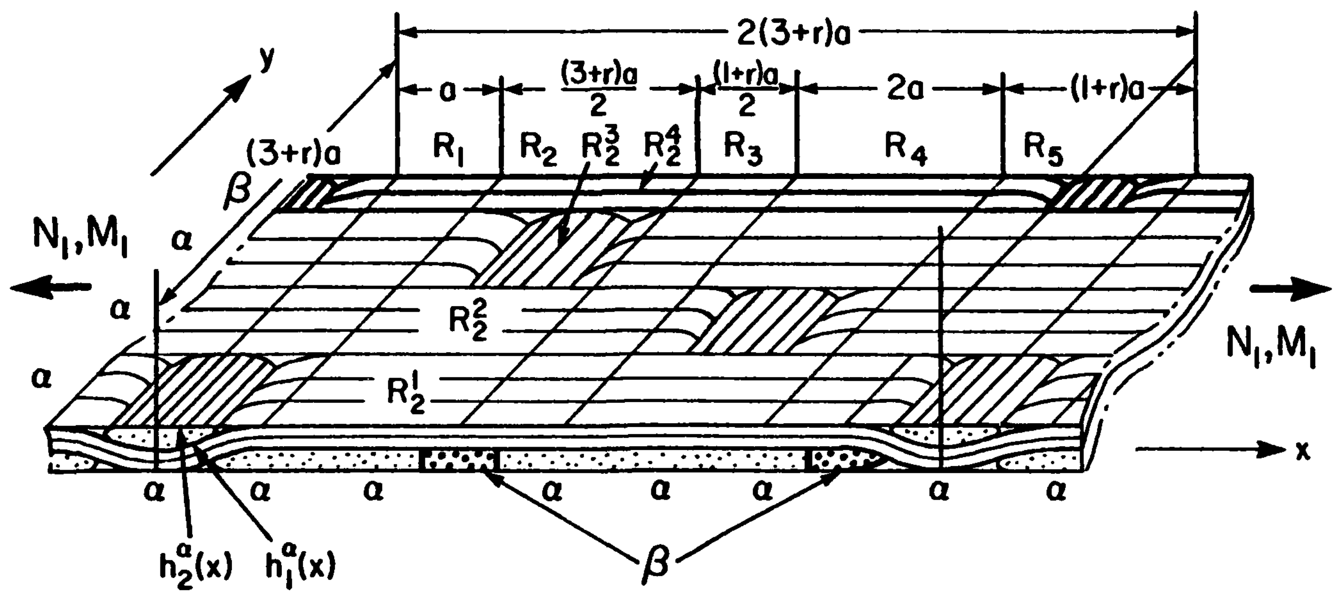

2(3+r)a
a
(3+r)a/2
(1+r)a/2
2a
(1+r)a
R1 R2 R2^3 R2^4 R3 R4 R5
(3+r)a
y
β
N1,M1
α
R2^2
R2^1
x
h2^α(x) h1^α(x)

Fig. 12d

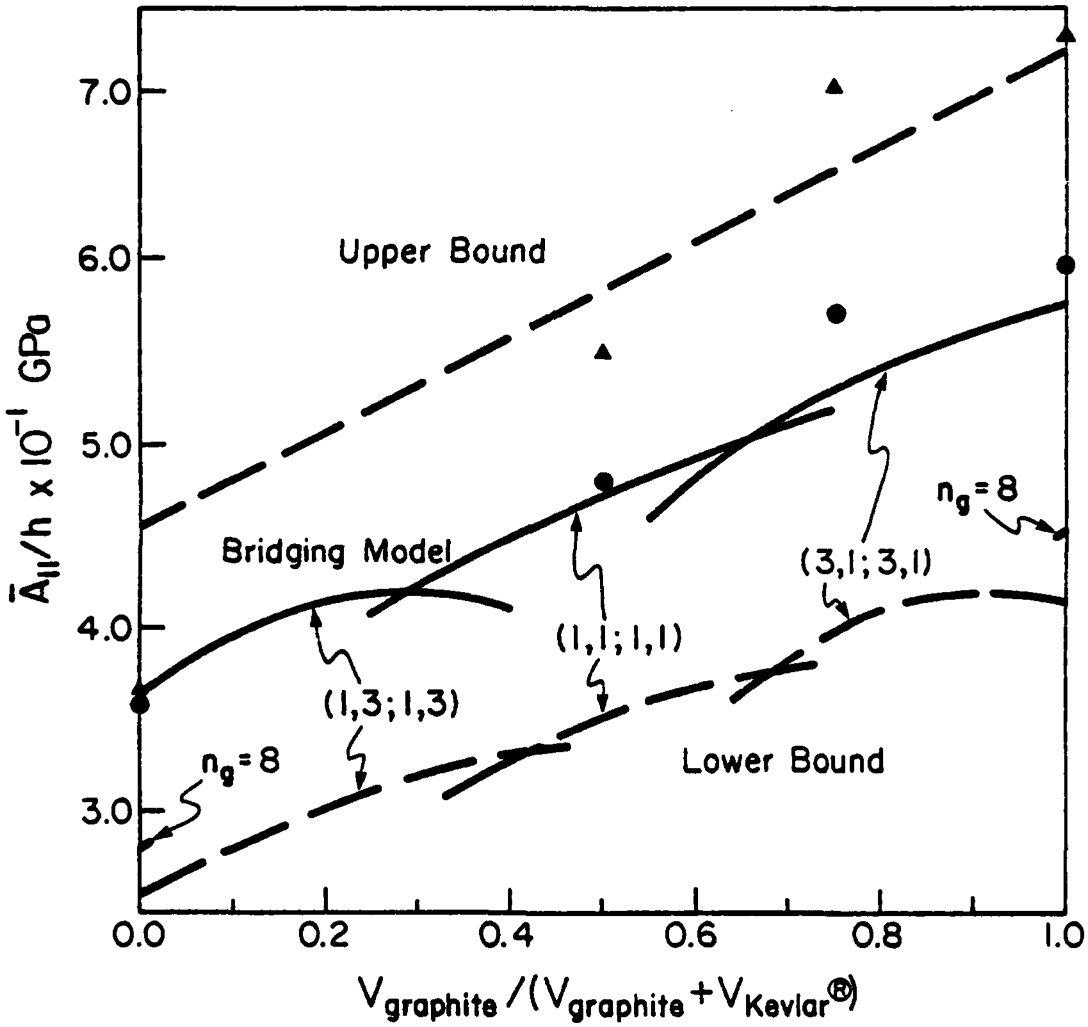
Upper Bound
Bridging Model
Lower Bound
(1,3;1,3)
(1,1;1,1)
(3,1;3,1)
$n_g = 8$
$n_g = 8$
$\bar{A}_{11}/h \times 10^{-1}$ GPa
$V_{graphite}/(V_{graphite}+V_{Kevlar^{®}})$
7.0
6.0
5.0
4.0
3.0
0.0
0.2
0.4
0.6
0.8
1.0

Fig. 13

FILME

4-84